Shear stress stimulates integrin β1 trafficking and increases directionalmigration of cancer cells via promoting deacetylation of microtubules

Kai Tang[a,1], Shun Li[a,c,1], Ping Li[a], Qiong Xia[a], Rui Yang[a], Tingting Li[a,c], Li Li[a,c], Ying Jiang[a,c], Xiang Qin[a,c], Hong Yang[a,c], Chunhui Wu[a,c], Fengming You[b], Youhua Tan[d,e], Yiyao Liu[a,b,*,**]

[a] Department of Biophysics, School of Life Science and Technology, University of Electronic Science and Technology of China, Chengdu 610054, Sichuan, PR China

[b] Hospital of Chengdu University of Traditional Chinese Medicine, No. 39 Shi-er-qiao Road, Chengdu 610072, Sichuan, PR China

[c] Center for Information in Biology, University of Electronic Science and Technology of China, Chengdu 610054, Sichuan, PR China

[d] The Hong Kong Polytechnic University Shenzhen Research Institute, Shenzhen, PR China

[e] Department of Biomedical Engineering, The Hong Kong Polytechnic University, Hong Kong, PR China

Running title: Integrin trafficking regulates flow-induced migration

*** Corresponding author at: School of Life Science and Technology, University of Electronic Science and Technology of China, Chengdu, Sichuan, PR China.**

**** Corresponding author at: Hospital of Chengdu University of Traditional Chinese Medicine, Chengdu, Sichuan, PR China.**

E-mail address: liuyiyao@uest.edu.cn (Y. Liu).

[1] **These authors contributed equally to this work**

List of Abbreviations

FA: focal adhesion

LSS:low shear stress

FRAP: Fluorescence recovery after photobleaching

Cav-1: caveolin-1

MTs: microtubules

CTCs: circulating tumor cells

ROCK: Rho-associated protein kinase

FBS: fetal bovine serum

MesNa: 2-mercaptoethane sulfonate

PQ: primaquine

IAA: iodoacetamide

MDC: monodansylcadaverine

PBS: phosphate buffer saline

GEO: Expression Omnibus database

FACS: fluorescence-activated cell sorting

FAK: Focal adhesion kinase

Abstract

In egress routes of malignancy, cancer cells are constantly subjected to shear stress imposed by blood/lymph flow. Increasing evidence points toward the regulatory roles of shear stress in tumor cell adhesion and motility. Although it is known that integrin endocytic trafficking governs focal adhesion (FA) turnover and cell migration, the effect and biological consequences of low shear stress (LSS) on integrin trafficking remain unclear. Here, we identified the critical role of integrin β1 trafficking and caveolin-1 (Cav-1) mediated endocytosis in LSS-induced cell directional migration. LSS altered the distribution of integrin β1 in MDA-MB-231 cells and significantly promoted its internalization and recycling, which in turn facilitated FA turnover and directional cell migration. Furthermore, LSS induced cytoskeleton remodeling, which was required for internalization of integrin β1. LSS down-regulated the acetylation level of microtubules (MTs) via activating ROCK/HDAC6 pathway, resulting in elevation of MTs dynamics, Cav-1 motility, and Cav-1-dependent integrin β1 recycling. We also showed that high HDAC6 expression was a ROCK-dependent prognostic factor, which was correlated with poor outcomes in breast cancer patients. Taken together, these results defined a novel mechanism by which LSS enhanced integrin β1 trafficking via actin cytoskeleton remodeling and ROCK/HDAC6 mediated deacetylation of MTs, thereby promoting FAs turnover and directional cell migration.

Keywords: Integrin internalization and recycling; Caveolin-1; Focal adhesion turnover; Microtubule deacetylation; HDAC6

1. Introduction

Metastasis is a complex series of sequential processes, leading to more than 90% of cancer mortality. Tumor cells disseminate from the primary site to distant metastatic sites mainly through vascular networks, including blood and lymphatic systems. Once intravasating into the circulatory system, tumors cells experience shear force from blood/lymph flow [1]. Biophysical cues, such as extracellular matrix stiffness and biomechanical forces, have been demonstrated to play important roles in intrinsic tumor cell biology and malignancy. Abundant evidence indicates that flow-induced mechanical forces are involved in modulating metastatic progression. The arrest and extravasation of circulating tumor cells (CTCs) tend to occur under relatively low shear stress (LSS) condition rather than high shear stress condition [2]. LSS has attracted significant attention for their roles in facilitating the arrest and extravasation of CTCs [3, 4]. More recently, our findings, together with others, showed that LSS directly impacted the motility and migration abilities of tumor cells [5, 6]. However, the mechanotransduction pathway and the mechanisms underlying how LSS influences cancer cell motility remain unclear.

Tumor cell migration relies on orchestrated turnover of integrin-based focal adhesions (FAs) [7]. FAs are dynamically disassembled at the rear of the cells and reassembled at cell front, which are spatiotemporally controlled by endocytic trafficking of integrins. Integrins undergo continuous internalization from the cell surface into endosomal compartments via clathrin- or caveolin-dependent endocytosis and then may be degraded or recycled back to the plasma membrane [7, 8]. There is clear evidence that the endo/exocytic traffic of integrins is crucial to cell migration and maintenance of a felicitous balance between intracellular and cell surface integrins [9]. The factor facilitating integrin endocytosis and recycling contributes to FA dynamics and integrin-mediated cell migration. Multiple biochemical factors can regulate cellular processes by altering integrin trafficking, such as TNF-α and growth factor [10]. Emerging

evidence points to more general roles of mechanical signals in regulating integrin endocytic trafficking. Extracellular matrix elasticity, an important mechanical stimulus, has been found to affect integrin activity and trafficking and modulate multiple cellular behaviors[11]. Integrin β1 is significantly activated and the endocytosis of integrin β1 is enhanced via caveolin-dependent endocytosis route on soft substrates, which influences stem cell lineage specification [12, 13]. Despite recent significant advancements, whether and how shear flow-induced mechanical forces regulate integrin trafficking and tumor cell metastasis have not been well addressed.

Cytoskeleton is essential in the regulation of various cell behaviors, including intracellular vesicle transport. Actin has been implicated in the endocytosis in several polarized tissue cell types, such as endothelial cells [14]. The depolymerization and rearrangement of actin cytoskeleton are required for endocytosis to form endocytic vesicles. Rho GTPase, a family of small signaling G proteins, plays a critical role in vesicle trafficking through regulating actin dynamics. Rac and Cdc42 are reported to modulate clathrin-dependent and caveolin-dependent endocytic processes and also contribute to intracellular vesicle sorting and transport [15, 16]. Microtubules (MTs) are the main transport track for endocytic vesicles in cells, especially for long-distance cargo transport. It is shown that the regulation of MT-dependent transport depends not only on the MT-associated motor proteins but also on the MT post-translational modifications, including acetylation and detyrosination [17, 18]. Tubulin modifications can affect the affinity of different kinds of MT-associated motor proteins to MTs and also regulate the velocity and processivity of motor proteins [19].

Here, we aim to investigate whether and how integrin trafficking is involved in the regulation of FAs turnover and tumor cell motility in response to LSS. In the present study, we demonstrate that LSS facilitates Cav-1 redistribution and integrin β1 trafficking by Rho-associated protein kinase (ROCK)-mediated actin cytoskeleton reorganization and MTs deacetylation, which promotes FAs

turnover and directional cell migration. These findings suggest that disruption of endocytosis and integrin trafficking to LSS exposure may hold therapeutic potential in inhibiting tumor cell motility. Our study discovers a new regulatory role of ROCK in dual control of integrin trafficking by microtubules and the actin cytoskeleton.

2. Materials and methods

2.1 Antibodies and reagents

Cell culture medium of L15, penicillin, streptomycin and fetal bovine serum (FBS) were purchased from Gibco (Grand Island, NY, USA). Monoclonal antibodies against caveolin-1 (Cav-1), acetyl-α-tubulin (Lys40), polyclonal antibodies against clathrin heavy chain, phospho-FAK (p-FAK; Tyr^{397}) and phospho-Paxillin (p-Paxillin, Tyr^{118}) were purchased from Cell Signaling Technology (Beverly, MA, USA). Monoclonal antibodies against integrin β1 were from BD Transduction Laboratories™ (San Jose, CA, USA) and Abcam (Cambridge, UK). Monoclonal antibody against β-actin and α-tubulin, polyclonal antibodies against HDAC6 were purchased from Proteintech Group (Rosemont, IL, USA). EZ-Link Sulfo-NHS-SS-Biotin was from Thermo Fisher Scientific (Waltham, MA, USA). Nystatin and ROCK inhibitor (Y27632) was purchased from Selleckchem (Houston, TX, USA). HDAC6 inhibitor (Tubastatin-A) was from MedChemExpress (Monmouth Junction, NJ, USA). TRTIC-conjugated phalloidin, 2-mercaptoethane sulfonate (MesNa), primaquine (PQ), iodoacetamide (IAA) and monodansylcadaverine (MDC) were purchased from Sigma-Aldrich (St. Louis, MO, USA). All other reagents were used as received without additional purification unless otherwise noted.

2.2 Cell culture

The triple negative human breast cancer cell MDA-MB-231 (ATCC HTB-26) was given by Dr. Jun Zhou (Nankai University, China). Cells were cultured in

L15 medium which contain 10% FBS, 1% penicillin and streptomycin. The culture condition was 37°C CO_2 incubator.

2.3 Parallel flow chamber system

A parallel flow chamber was developed to exert the laminar shear force on the cells as described previously [5, 20]. The laminar shear force (τ) is related to the volumetric flow rate (Q) and calculated by $\tau=6\mu Q/w(h)^2$, where μ = 0.0007 Pa·s is the dynamic viscosity of medium at 37°C, *w* is the width of the flow field, and h is the height. The shear stress imposed to cells can vary from 0.5 to 37 dyn/cm^2 through altering the flow rate of Q, which mimic the physiological shear stress occurring in different parts of the human blood flow. The flow rate of Q was controlled by a peristaltic pump.

2.4 Immunofluorescence staining

Cells seeded on glass coverslips were fixed with 4% paraformaldehyde in phosphate buffer saline (PBS) for 15min at room temperature and permeabilized with 0.1% for 10min, and blocked with 1% BSA in PBST (1×PBS, 0.1% Tween-20) for 1h. Cells were incubated with indicated primary for overnight at 4°C and stained with Alexa-conjugated secondary antibodies for 1h at room temperature. After washed 3 times in PBST for 5min, samples were visualized on a confocal laser scanning microscope (FV1000, Olympus, Japan). The fluorescence intensity and colocalization calculation of confocal images were analyzed by using ImageJ software (NIH, USA).

2.5 Flow cytometry

To analyze the surface expression of integrin β1, cells were collected by trypsinization and washed in rinsing buffer (1×PBS, 2 mM EDTA, 0.5% BSA), then resuspended in 4% paraformaldehyde for 15 min at 4°C, washed 3 times in PBS and resuspended at 1×10^6 cells/mL in rinsing buffer. Cells were incubated at 4°C for 1h with anti-integrin β1 antibody, washed 3 times and

incubated with ALexarFluor 488-labeled secondary antibody for 1h in dark. Cells were then washed 3 times again in rinsing buffer, and the mean fluorescence intensities were measured using a flow cytometer (FACS Calibur, BD, USA).

2.6 Western blot analysis

RIPA lysis buffer (Beyotime, China) was used for cell lysis. Proteins were extracted by 10% SDS-PAGE and followed with electrotransferred with PVDF membranes (Millipore; Billerica, MA, USA). Blocking solution (5% non-fat dry milk in TBST which included 10 mM Tris-HCl, 100 mM NaCl, 0.1% tween-20) was used for preventing nonspecific binding by 1h incubation in room temperature. Primary antibodies were diluted in 1:1000 for overnight incubation. After washing, incubation with corresponding secondary antibody at 37°C for 1h. By following the instruction of ECL and ECL Plus (Beyotime) immunoreactive bands were showed and β-actin was used for protein normalized.

2.7 Integrin internalization, recycling and degradation assays

The fresh L15 medium was used to stimulate the cells for 1h incubation before the assay. After twice of cold PBS washing, cells were labeled by NHS-SS-biotin (200 μg/mL) at 4°C for 30min. Integrin internalization, recycling and degradation assays were conducted according the previous literature [9]

For internalization, the L15 medium with 0.6 mM primaquine (PQ) was used for cell incubation at 37°C for indicated time points. The washing step was repeated twice with ice-cold PBS and a cleaning solution (included 20 mM MesNa (a non-cell-permeant reducing agent), 50 mM Tris at pH 8.6, 100 mM NaCl) was used to remove the remaining biotin on cell surface by 15min raising at 4°C. The addition of 20 mM IAA was used for quenching the MesNa by 10min incubation at 4°C. The capture-ELISA was used to quantify the biotinylated integrin β1. In non-MesNa-treated samples were used to determine the total

surface biotinylated integrin β1 protein of the cells and the cytoplasm protein was quantified in proportion toward it.

For recycling assays, by 15min absence of primaquine, internalization was performed. After washing with PBS, the MesNa was used to remove the remaining cell-surface biotin. To remove the biotin from recycled protein, MesNa was used to quench with 20 mM iodoacetamide for secondary reduction. This step was for detecting degradation of the internal pool. After washing twice in PBS, cells were lysed. Capture-ELISA was used to quantify the biotinylated integrin β1.

The cells with NHS-SS-biotin labeled were firstly transfer into L15 medium at 37°C and then lysed the cells at corresponding time points in order to quantify the integrin degradation. Capture-ELISA was used to quantify the biotinylated integrin β1. The degradation value was calculated by dividing the total surface biotinylated integrin β1 and express in percentage.

2.8 Capture-ELISA

The ELISA plates were purchased from Cusabio (Wuhan, China) with certain antibodies of integrin β1. After adding cell lysates to the plate, 2h incubation in 37°C was carried out. Plate was washed with washing buffer and incubated with HRP-streptavidin for 1h in 37°C. Another washing step was carried out and followed by TMB substrate incubation for 20min in the dark for showing the biotinylated proteins. Stopping solution was used to terminate the showing reaction. A microplate reader (Model 680, Bio-Rad; Philadelphia, PA, USA) was used to determine the absorbance in 450 nm wavelength of light.

2.9 Plasmids and transfection

Cells were trypsinized and quantified before plating on a glass with 0.5 mL of complete growth medium. The cell density should be controlled in between 50-80% confluent for transfection. Lipofectamine LTX® Reagent (Invitrogen; Carlsbad, CA, USA) was used as transfected source for $1.25x10^5$ of cells and

followed the instruction of the company. For cell transfection, 0.5 μg of DNA were diluted in 100 μL of Opti-MEM® I Reduced Serum Media without serum. Then 0.5 μL of PLUSTM Reagent was mixed and added into target DNA solution and followed by 15min of incubation in room temperature. The DNA-Lipofectamine LTX® Reagent complexes was made from 1.25-2.25 μL of Lipofectamine LTX® Reagent and Opti-MEM® DNA solution by 30min incubation in room temperature. After incubation, reagent complexes are added the reagent complexes into the plate (100 μL per well) and placed the plate on shaking table for mixing gently. After transfection, 18-24h normal incubation was carried out for the cells (in 37°C, 5% CO_2 incubator) and then determined the transgene expression. EGFP-tubulin plasmid was a kind gift from Prof. Guillaume Montagnac (Gustave Roussy Institute, France). RFP-caveolin-1 was a generous gift from Prof. Richard D. Minshall (University of Illinois at Chicago, USA).

2.10 Time-lapse video microscopy

In order to track the cell migration, a 200 mL pipette tip was used to create a wound on the confluent monolayer cells. Before treated with LSS, cells were washed with PBS for twice. LSS was set for 0 min (control), 2h post scraping (testing group). Nikon TE-2000U (Tokyo, Japan) was used to monitor the cell migration under the microscope, the whole equipment was set in 37°C incubator. ImageJ software was used for data analysis.

The plasmid EGFP-vinculin was transiently transfected into cells for FA dynamics evaluation and the cells were cultured for 24-36h. Confocal laser scanning microscope (FV1000, Olympus, Japan) was used for imaging. For recording the cell behaviors, images were captured every 30s for 10min. Image J was used to generate the Kymographs.

The plasmid EGFP-tubulin was transiently transfected into cells for MT dynamics evaluation. Confocal laser scanning microscope (FV1000, Olympus, Japan) was used for imaging. For recording the cell behaviors, images were

captured every 10s for 3min. Catastrophe frequency was calculated by dividing the number of MT catastrophes events by the total time of observation. Rescue frequency was calculated by dividing the number of MT rescues events observed by the total time.

2.11 Fluorescence recovery after photobleaching (FRAP) analysis

Cells were transfected with the plasmid RFP-caveolin-1 and imaged with the confocal laser scanning microscope (LSM 710, Carl Zeiss, Germany). Before bleaching, five images were taken for control. The 561 nm line argon of the nominal 100% laser transmission was used for 5 times bleaching. Under the low laser power, recording images were taken at every 2s for 5min. Image J was used for data analysis

2.12 HDAC6 activation and acetyltransferase activity assays

HDAC6 activation and acetyltransferase activity assays were conducted according to our previously published literature report with minor modifications [21]. MDA-MB-231 cells were treated with 10 μM of TBA for 16h for quantifying the HDAC6 activity. All the reaction was done in complete growth medium as it guaranteed that the MT acetylation was in maximum which was also confirmed by western blotting and immunofluorescence. The complete growth medium was used to wash out the inhibitor contained medium. The cells were placed into static (control) or LSS (test) condition for corresponding time points. To validate the cell lysates, Western blotting was used right after each the incubation. The final value of the acetylated α-tubulin under each condition was calculated by dividing the band intensity of each condition toward the control one.

2.13 Kaplan-Meier survival analysis

The GSE25066 microarray expression profile was collected from Gene Expression Omnibus database (GEO, http://www.ncbi.nlm.nih.gov/geo/). The

fitting targets were the patients who had breast cancer and were treated with chemotherapy drugs (taxane, anthracycline). All the selected data were analyzed by the R_2 microarray public database (http://r2.amc.nl) or GraphPad Prism Software version 6.0.

2.14 Statistical analysis

To eliminate the error, each experiment was repeated at least three times. Data were performed in means ± SD. *t*-test was used for analyzing the data and $p<0.05$ was used to determine the statistically significant difference. The p-value of Kaplan-Meier survival analysis was calculated by log-rank test. Results were analyzed by GraphPad Prism software 6.0.

3. Results

3.1 LSS promotes integrin β1 internalization and recycling in MDA-MB-231 cells

Extracellular matrix elasticity is reported to affect integrin trafficking and reduce surface integrin levels, which modulate the fate and function of bone marrow mesenchymal stem cells [12,13]. These findings led us to investigate the effect of LSS on integrin β1 distribution and trafficking in MDA-MB-231 breast cancer cells. First, we explored the subcellular distribution of integrin β1 after exposing cells to LSS for different durations (0, 0.5, 1, and 2 h). Integrin β1 was labeled by AlexaFluor 594 (red). Immunostaining analysis showed that integrin β1 predominantly localized to the plasma membrane in the static condition. After 0.5 h of LSS exposure (1.8 dyn/cm2), integrin β1 showed punctate-like distribution throughout the cell. Then integrin β1 was highly enriched in a perinuclear compartment after 1 h of LSS exposure. Interestingly, following the exposure to LSS for 2 h, the amount of integrin β1 localizing to perinuclear compartment decreased significantly (Fig. 1A). We further measured the levels of integrin β1 expression on cell surface using

fluorescence-activated cell sorting (FACS) analysis. The results showed that LSS exposure for 0.5 h and 1 h resulted in up to 50% decrease in the amount of integrin β1 on the cell surface, whereas surface integrin β1 returned to the normal level after 2 h of LSS exposure (Fig. 1B and C). The change of integrin β1 distribution may be caused by the expression or trafficking of integrin β1. We next investigated whether the obvious differences of integrin β1 subcellular distribution after LSS exposure were due to variations in total protein levels. Cells were kept under static condition as control or exposed to LSS, and the total expression of integrin β1 was examined by Western blotting. The total cellular content of integrin β1 was not significantly altered by LSS (Fig. 1D and E). These results indicate that LSS might alter the distribution of integrin β1 through its trafficking, but not total protein expression

Focal adhesion kinase (FAK) has been associated with both FA assembly and disassembly. The phosphorylation of tyrosine 397 in FAK is essential in promoting FA turnover [22]. In this study, we found that LSS rapidly increased the FAK phosphorylation on Y397 (Fig. 1D and E), suggesting that LSS is involved in regulating FAs turnover in MDA-MB- 231 cells. However, further study is required to provide more convincing evidence.

To further validate whether integrin β1 trafficking is modulated by LSS, we used a biotin-labelling and capture-ELISA protocol to quantify the kinetics of integrin β1 trafficking (Fig. S1). The data showed that LSS exposure was able to accelerate both the internalization rate (Fig. 1F) and recycling rate (Fig. 1G) of integrin β1 compared with the static group. Interestingly, we found that the percentage of internalized integrin β1 at 30 min was higher than that at 60 min and 120 min in both static condition and LSS exposure. We supposed that some of internalized biotinylated-integrin β1 had been recycled back to the plasma membrane and that the biotin was reduced by MesNa treatment. To investigate whether LSS affect the degradation of integrin β1, we used biotin to label integrin β1 on the cell surface and incubated cells in complete medium to allow for internalization and recycling. As shown in Fig. 1H, the kinetics of integrin β1

degradation in static condition were similar to that in LSS exposure. We examined the net internalization of integrin β1 after treating cells with primaquine, an endosomal recycling inhibitor [9,23]. Compared to the static group, LSS exposure increased the concentration of net internalized integrin β1 (Fig. 1I). Taken together, these data support that LSS accelerates integrin β1 internalization and recycling, without affecting integrin β1 degradation.

3.2 LSS accelerates clathrin-independent integrin β1 internalization

Integrins were reported to undergo trafficking through clathrin and/ or caveolin pathways [7–9]. However, the same integrin may use multiple pathways for internalization [24,25]. To investigate the pathway through which LSS regulates integrin β1 internalization, we performed experiments with compounds that specifically block diverse endocytosis routes. We pretreated cells with cholesterol-depleting drug nystatin or inhibitor of clathrin-dependent endocytosis monodansylcadaverine (MDC) and then measured the net internalization of integrin β1 by biotin-labelling and capture-ELISA. Compared to LSS group, both nystatin and MDC treatment groups notably decreased the net internalization of integrin β1 (Fig. 1I), suggesting that both clathrin dependent and independent pathways are involved in LSS-mediated integrin β1 internalization. Further, the net internalization of integrin β1 was attenuated more by nystatin treatment than by MDC treatment, suggesting that the clathrin-independent endocytosis may play more important roles than the clathrin pathway in mediating LSS-induced integrin β1 internalization (Fig. 1I).

As an important way of clathrin-independent integrin internalization, we further investigated the role of Cav-1 in LSS-induced integrin β1 internalization by immunofluorescence staining. The results showed that more Cav-1 was quickly (after 15 min) colocalized with integrin β1 at the plasma membrane of LSS exposure (Fig. 2A, C and Fig. S2A). Following the exposure to LSS for 30 min, the colocalization of Cav-1 and integrin β1 was further enhanced and detected in intracellular compartments (Fig. 2A and C). By contrast, no

significant colocalization of clathrin and integrin β1 was observed following LSS exposure (Fig. 2B, C and Fig. S2B). Integrin activation is required for the regulation of multiple cell behaviors, such as cell polarity, migration, cell cycle progression, adhesion, and survival [26–29]. We next examined the colocalization of Cav-1 and active integrin β1 by using conformation-sensitive antibodies against the active integrin β1. At 30 min after LSS exposure, the 3D reconstruction images showed that active integrin β1 was colocalized with Cav-1 in the perinuclear endocytic recycling compartment (Fig. 2D and E). These results indicate that LSS promotes integrin β1 internalization via a clathrin-independent endocytosis (might be Cav-1 mediated endocytosis) mechanism.

3.3 LSS induced integrin β1 internalization is required for directional cell migration, FAs disassembly and polarized assembly

Coordinated trafficking of integrin is required for efficient cell migration [30]. We have previously reported that Cav-1 mediates multiple downstream signaling pathways triggered by LSS to regulate MDA-MB 231 cell motility [5,31]. We thus further investigated whether caveolindependent integrin internalization affects cancer cell migration. Consistent with our previous work, LSS exposure enhanced cell track length and mean velocity (Fig. 3A and C). We also found that LSS increased other cell migration associated parameters, including instant velocity (Fig. 3B), Euclidean distance (Fig. 3D), and directionality of migration (expressed as cells that move within a 60° angle from the starting point) (Fig. 3F), but not directionality ratio (expressed as the ratio between net and total distance, Fig. 3E). These results support the idea that LSS exposure favors cancer cell directional migration. Inhibiting caveolin by nystatin pretreatment resulted in notable decrease in cell track length, the instant and mean velocity, Euclidean distance, persistency, and directionality of migration. These data demonstrate that Cav-1- dependent internalization is essential for LSS-induced directional cell migration.

Spatio-temporal regulation of FA turnover plays a key role in coordinating

cell migration [32]. Endo-exocytic integrin trafficking is reported to regulate FA turnover [33]. We have shown that LSS induces integrin β1 trafficking, FAK phosphorylation, and cell migration. It is possible that LSS may enhance FA turnover through regulating integrin trafficking and thereby promote cell migration. To test this idea, we examined the effect of caveolin-dependent internalization on FA disassembly of cells expressing GFP-vinculin. Our data show that LSS facilitated FA disassembly compared to cells in static condition (Fig. 3G, H and Movie S1). Pretreatment with nystatin inhibited LSS-induced FA disassembly. Next, we examined FA polarized assembly in cells at the edge of a wounded monolayer. We found that FA assembly was highly polarized toward the leading edge after LSS exposure. Importantly, LSS failed to promote FA polarized assembly at the leading edge after nystatin pretreatment (Fig. 3I). We also examined the localization of Cav-1 and active integrin β1 in FAs in both static and LSS-exposed cells by immunofluorescence staining. The results showed that active integrin β1 was found in FAs, whereas Cav-1 expression was weak in static cells. After the exposure to LSS for 15 min, much more Cav-1 was recruited to cell edge next to the FAs (Fig. 3J). These results suggest that LSS promotes Cav-1 redistribution, FA disassembly, and polarized assembly might through regulation of integrin β1 internalization.

3.4 LSS-induced decreased acetylation of tubulin and actin cytoskeletal reorganization are required for integrin β1 internalization

It has been reported that actin and MT are involved in regulating caveolae dynamics and endo-exocytic trafficking [34–36]. Moreover, we have demonstrated previously that LSS induces cell cytoskeletal reorganization through ROCK/p-MLC pathway [5]. Therefore, we wondered whether LSS modulated Cav-1 redistribution and integrin β1 trafficking through the effects on the organization and/or function of actin and MT cytoskeleton. Our data show that LSS significantly decreased cellular MT acetylation compared to static cells (Fig. 4A and B), which was further confirmed by Western blotting analysis (Fig.

4C). In addition, stress fibers were disrupted after LSS exposure for 30 min. However, F-actin was repolymerized to form new stress fibers which were organized in bundles along the long axis in cells exposed to LSS for 1 h and 2 h (Fig. 4A).

Actin cytoskeleton plays a key role in regulating caveolae endocytosis [37]. To explore the link between LSS-induced actin cytoskeleton rearrangement and caveolin-dependent integrin β1 internalization, cells were pretreated with ROCK inhibitor Y-27632 and loaded with LSS. The results showed that inhibiting ROCK prevented LSS-induced actin rearrangement and the colocalization of Cav-1 and active integrin β1 (Fig. 4D and Fig. S3). Furthermore, Cav-1 appeared peripheral but not perinuclear accumulation following LSS exposure (Fig. 4D). We adopted biotin-labelling and capture-ELISA to measure internalization of integrin β1 and found that Y-27632 pretreatment inhibited LSS-induced integrin β1 internalization (Fig. 4E). Taken together, our data demonstrate that ROCK-mediated actin cytoskeleton rearrangement is essential for LSS-induced Cav-1 redistribution and integrin β1 internalization.

3.5 LSS-induced tubulin deacetylation enhances MT dynamics, Cav-1 motility, and integrin β1 recycling

It is widely reported that the acetylation level of tubulin is associated with the dynamics and stability of MT, which regulates vesicles transport and cell migration [21,38]. We found that there were thick and disordered MT bundles at the periphery of static cells. LSS exposure induced the formation of abundant thin microtubule filaments extending to the leading edge at the cell front (Fig. 5A, B and Movie S2). Bundling of MTs often increases the stability of MTs [39]. To visualize the effect of LSS exposure on MT dynamics, we performed time-lapse photography analysis in EGFP-tubulin-transfected cells. Live imaging showed that MTs in static cells were highly stable, whereas LSS promoted MT catastrophe and reduced the duration between phases of growth and

shortening (Fig. 5A and Movie S2), suggesting that LSS enhances MT dynamics. Moreover, more Cav-1 was recruited to peripheral MTs at the leading edge of cells after LSS exposure (Fig. 5B and Fig. S4).

Cav-1-containing vesicles move along MT tracks and the transport can be modulated by MT dynamics [36]. Thus, we further explored the effect of LSS-induced tubulin deacetylation on Cav-1 mobility and integrin β1 trafficking. We inhibited tubulin deacetylation by treating cells with Tubastatin-A (TBA), an inhibitor of microtubule deacetylase HDAC6. The results of FRAP analysis showed that LSS facilitated the recovery of RFP-Cav-1 fluorescence signal after bleaching, indicating the increase in the mobility of Cav-1 in LSS-exposed cells. However, the mobility of RFP-Cav-1 was considerably inhibited by blocking tubulin deacetylation (Fig. 5C, D and Movie S3). We also quantified the trafficking of integrin β1 by using biotin-labelling and capture-ELISA. The data show that inhibiting tubulin deacetylation had no effects on LSS-induced integrin β1 internalization (Fig. 5E). Notably, TBA treatment inhibited LSS-induced increase in integrin β1 recycling but not degradation (Fig. 5F and G). Collectively, these findings demonstrate that LSS exposure enhances MT dynamics, Cav-1 motility, and integrin β1 recycling via tubulin deacetylation.

3.6 ROCK-dependent activation of HDAC6 is required for LSS-induced MT deacetylation

MTs are reversibly acetylated by multiple acetyltransferases, whereas deacetylation of MTs is regulated by HDAC6 and Sirtuin 2 [40–42]. HDAC6 but not Sirtuin 2 has been demonstrated as the predominant tubulin deacetylase in MDA-MB-231 cells [21]. Thus, we hypothesized that LSS might promote MT deacetylation through downregulation of acetyltransferases or up-regulation of HDAC6. To assess the activity of acetyltransferases regulated by LSS, we measured the rate of α-tubulin acetylation by treating cells with HDAC6 inhibitor TBA. The results showed that there was no significant difference in tubulin acetylation between static and LSS-exposed cells (Fig. 6A and B). To explore

the role of LSS in HDAC6 activity, cells were pretreated with TBA to produce MT hyperacetylation and then removed in the static and LSS conditions. We found that the rate of α-tubulin deacetylation in LSS-exposed cells was notably higher than in static cells. These data demonstrate that LSS promotes MT deacetylation via enhancing HDAC6 activity (Fig. 6C and D).

We sought to further investigate how LSS regulates the activity of HDAC6. It has been shown that HDAC6 enzymatic activity may affect HDAC6 binding to MTs and regulate MT stability [43]. ROCK, a downstream effector of the Rho-GTPase signaling, is an important modulator of cytoskeletal dynamics and can regulate HDAC6 activity [44]. Thus, we examined whether LSS enhanced HDAC6 activity via ROCK. The result show that inhibiting ROCK significantly increased the level of MT acetylation but blocked LSS-induced MT deacetylation (Fig. 6E and F). Taken together, our data suggest that LSS promotes MT deacetylation via ROCK-dependent up-regulation of HDAC6 activity.

Since HDAC6 has been associated with metastasis in various cancers [42,45,46], we further investigated the correlation between HDAC6 and survival rates of breast cancer patients treated with taxane and anthracycline by analyzing GSE25066 dataset from the Gene Expression Omnibus (GEO). High expression of HDAC6 was found to be associated with poor survival probability in breast cancer patients treated with chemotherapy drugs ($p = 0.011$, Fig. 6G). We also examined whether HDAC6 expression could differentiate patients at different TNM stages. Based on GSE25066 dataset, the breast cancer patients were divided into early-stage (TNM I-II) and advanced-stage (TNM III-IV) groups. The results showed that patients with high HDAC6 expression showed significantly poor prognosis in both the early-stage subgroup ($p = 0.011$, Fig. 6H) and advanced-stage group ($p = 0.021$, Fig. 6I). We then investigated the relationship between ROCK expression, HDAC6 activity, and prognosis of breast cancer patients. The results showed that high HDAC6 expression was strongly correlated with poor prognosis in patients with high ROCK expression

(p = 0.0007, Fig. 6J). However, there was no significant difference in the survival probability of patients with low ROCK expression when HDAC6 was altered (Fig. 6J). These results identify high HDAC6 expression as a ROCK dependent prognostic factor, which predicts poor prognosis in breast cancer patients.

4. Discussion

Numerous studies have provided compelling evidence that integrin can respond to various biochemical and mechanical signals through endo-exocytic trafficking to regulate cellular functions. For example, TNF-α induces the internalization and recycling of integrin α5β1 and promotes the rapid redistribution of integrin on cell membranes [10]. It has been reported that extracellular matrix elasticity significantly enhances the activation and internalization of integrin to modulate the differentiation of bone marrow mesenchymal stem cells [12,13]. Fluid shear stress regulates various cellular functions, including integrin activation [47], cell migration [6], differentiation [48], and anoikis resistance [49]. However, the effect of LSS on integrin trafficking remained to be explored. Here, we demonstrate that LSS induces Cav-1-dependent integrin β1 trafficking that regulates FA dynamics and motility.

The endo-exocytic trafficking of integrin plays a pivotal role in controlling the distribution of integrin in migrating cells [50]. Our data indicate that LSS exposure accelerates the internalization and recycling of integrin β1 and induces integrin β1 redistribution without changing its overall expression. There are reports showing that long-term laminar shear stress (15 dyn/cm2 for 12 h) upregulates integrin α5β1 expression to facilitate the adhesion and survival of endothelial cells [51]. The difference in integrin expression could be due to the magnitude of shear stress, loading duration, and cell type. In general, integrin endocytosis is mainly mediated through clathrin-dependent and clathrin-independent pathways [9]. Clathrin-independent internalization routes include Cav-1-dependent endocytosis and macropinocytosis stimulated by growth

factors [8,52]. Our results show notable increase in colocalization of integrin β1 and Cav-1 but not clathrin in cells under LSS condition. Inhibiting clathrin-independent endocytosis pathway suppresses the net internalization of integrin β1 more than inhibiting clathrin endocytosis pathway. It was previously shown that the endocytosis of integrin β1 is dynamin and clathrin dependent [9]. In contrast, Polina and co-workers showed that integrin β1 is trafficked mainly via a Cav-1-dependent route in the metastatic breast cancer cells [8]. Different heterodimers of integrin β1 can colocalize with different endocytosis machinery structures [53], which might well explain the argument of the internalization route of integrin β1. Coordinated FA assembly and disassembly are required for cell migration.

It has been reported that shear stress induced FA remodeling and FA dynamics (assembly and disassembly) are determined by shear flow conditions in epithelial and endothelial cells [54,55]. Our results show that LSS enhances the rate of FA disassembly and promotes polarized FA formation in the leading edge of MDA-MB-231 cells, thus enhancing cell motility. Integrin endocytic recycling has been linked to cell migration through FA dynamics in a dynamin- and clathrin-dependent manner [7]. In spite of playing critical role in tumorigenesis and metastasis of liver, prostate [56], colon [57], breast, kidney, and lung cancers, Cav-1 could regulate cancer cell chemotherapy resistance through caveolae-mediated endocytosis [58]. Cav1 Tyr14 phosphorylation is a critical factor of tumor progression, which could promote caveolin scaffolding domain-dependent focal adhesion traction, cancer cell migration and invasion [59,60]. Caveolae internalization is increased upon the phosphorylation of Cav-1 at Tyr14, which leads to caveolin-dependent ligand-integrin endocytosis [8]. Our previous work shows that Cav-1 and the phosphorylation of Cav-1 at Tyr14 are essential for LSS-induced cell motility and metastasis [5,31]. Here, we further investigated whether Cav-1 redistribution and integrin β1 internalization is required for LSS-induced FA dynamics and cell motility. We show that Cav-1 is colocalized with active integrin β1 closed to FAs under shear flow. Our

findings are consistent with the fact that Cav-1 is recruited to the cellular periphery by activated Rac1 and accumulates at FAs, which triggers series of events that involve FA turnover and endosomal trafficking [61]. Taken together, our data identify Cav-1 as a novel regulator of FA dynamics that mediates LSS-induced integrin β1 internalization.

We show that LSS down-regulates MT acetylation and reorganizes actin cytoskeleton, which are consistent with previous studies [5,31,55,62]. Cell cytoskeleton is essential for various cellular events including endocytosis and intracellular cargo trafficking. The endocytosis of caveolae is highly dependent on actin cytoskeleton, as stress fiber regulators, Abl kinases or mDia1, are required for the relocalization of Cav-1 from the plasma membrane to the perinuclear region [63]. An intact and dynamic actin cytoskeleton is essential for caveolae internalization. We determine the correlation between LSSinduced actin cytoskeleton reorganization and Cav-1-dependent integrin internalization. Our data show that inhibiting ROCK-mediated cytoskeletal reorganization not only blocks LSS-induced colocalization of Cav-1 and active integrin β1, but also retards LSS-induced internalization of integrin β1. These findings might hint the roles of actin cytoskeleton in Cav-1-mediated endocytosis. Our results further validate a working model proposed previously, in which caveolae remain static by being anchored to actin cytoskeleton, whereas stress fibers reorganized by various stimuli would pull caveolae away from the plasma membrane into the cytoplasm, resulting in caveolae endocytosis [37].

The transition of MTs between growth phase and shrinkage is defined as dynamic instability, which plays a central role in cell polarity and adhesion turnover involved in intracellular trafficking [64]. Acetylation, a tubulin post-translational modification, is associated with stabilized MTs, can promote tumor cells migration [65], invadopodia activity and invasion [45]. In this study, our data show that LSS enhances MT dynamics, which may be due to LSS-induced MTs deacetylation. Endocytic caveolae are transported along MT tracks and fused with endosomal compartments, from where they can be recycled to the

plasma membrane. Previous studies show that bidirectional traffic of caveolae occurs on dynamic MTs, and that caveolar traffic can be enhanced by increasing MT dynamics [34,36]. Consistently, we show that LSS enhances Cav-1 motility and integrin β1 recycling, which can be blocked by inhibiting MT deacetylation. Collectively, our results suggest that LSS enhances MT dynamics by down-regulating MT acetylation, thus facilitating the recycling of Cav-1 positive vesicles containing integrin β1. Although MT dynamics have been known as a key determinant of caveolar trafficking, the mechanisms how MT dynamics regulates the transport of caveolae along MTs are poorly understood. Vesicle trafficking along MTs is driven by multiple molecular motors, including the families of dyneins and kinesins motor proteins [66]. Our data suggest that the activity of caveolae-associated motors is regulated by MT instability and/or posttranslational modification, which is supported by the findings that MT modifications affect the activities of diverse molecular motors. For example, kinesin KIF5c and KIF5B move preferentially on detyrosinated and acetylated MTs, respectively [17,67]. Tubulin deacetylation enhances KIF1C motility [18]. Nevertheless, further studies are needed to address whether LSS-induced MT deacetylation is able to influence caveolar trafficking by promoting the activity of molecular motors.

Acetylation of tubulin occurs on lysine 40 (K40) by multiple acetyltransferases and can be reversed by HDAC6 and SIRT2. Here we show that LSS significantly enhances the rate of HDAC6-dependent MT deacetylation but has no apparent effects on the activity of acetyltransferase. ROCK is a key modulator of cytoskeletal dynamics [67]. We have reported previously that LSS reorganizes the cytoskeleton through activating ROCK/p-MLC pathway [14]. It is shown that ROCK increases HDAC6 activity by inhibiting TPPP1/HDAC6 interaction and suppresses MT acetylation levels [44]. Our study demonstrates that LSS enhances HDAC6 activity and tubulin deacetylation in a ROCK-dependent manner.

In this study, we have found that ROCK and HDAC6 synergistically

regulated the Cav-1 dependent integrin trafficking to promote breast cancer cells migration. Previously, several studies showed that the expression of Cav-1 in invasion sites is higher than benign and in situ breast tumors [68,69]. High Cav-1 expression was reported as a poor survival marker in breast cancer patients. In addition, we have found that LSS enhanced Cav-1 motility via ROCK-HDAC6 pathway and high expression of HDAC6 was associated with poor survival probability in breast cancer patients [5]. Importantly, we have shown that high HDAC6 expression was strongly correlated with poor prognosis in patients with high ROCK expression but not in patients with low ROCK expression, suggesting that HDAC6 and ROCK inhibitor may be combined used as a prophylactic for preventing metastasis.

In summary, our study has provided compelling evidence that LSS promotes Cav-1 redistribution, FA dynamics and cell motility through regulation of integrin β1 trafficking. LSS facilitates the internalization and recycling of integrin β1 might in a caveolin-dependent manner, which promotes FA disassembly, FA polarized assembly, and cell migration. LSS-induced integrin β1 trafficking is mediated by cytoskeleton reorganization and MT deacetylation. Moreover, we identify ROCK as a key molecular switch that modulates cytoskeleton reorganization and HDAC6-mediated MTs deacetylation in response to LSS. Based on our findings, we propose a model to summarize the effect of LSS on integrin β1 trafficking in breast cancer cells (Fig. 7). LSS triggers ROCK-mediated actin cytoskeletal reorganization to facilitate caveolin-mediated integrin β1 internalization, which promotes FA turnover. LSS-activated ROCK/HDAC6 pathway enhances MT deacetylation and dynamics, Cav- 1 motility, and Cav-1-dependent integrin β1 recycling, which thenpromote FA dynamics and cell motility. Taken together, our study identities a novel role of integrin trafficking in LSS-induced FA dynamics and cell motility, thus providing a new target for the prevention of metastasis through the modulation of clathrin-independent integrin trafficking.

Conflict of interest

The authors declare that they have no competing interests.

Acknowledgments

This work was supported, in part or in whole, by the National Natural Science Foundation of China (U19A2006, 11772088, 11672255, 31700811, 11802056, 31800780, 11972111, 31900940, 81671821), the China Postdoctoral Science Foundation (2018M640904, 2019T120831), the Sichuan Science and Technology Program (2017JY0019, 2017JY0217, 2019YJC0183, 2019YJC0184), the Shenzhen Science and Technology Innovation Commission (JCYJ20170413154735522) and the Fundamental Research Funds for the Central Universities (ZYGX2019J117).

Author Contributions

K.T. S.L and Y.L initiated the project; K.T. S.L., X.Q., Y.J., H.Y., C.W. Y.T., F.Y. C.Z., J.Z. and Y.L. designed the experiments and analyzed the data; K.T., S.L., Y.C., Y.P., X.J., and Y.Z. performed all experiments; K.T, S.L., Y.T. and Y.L wrote the manuscript.

References

[1] Y.L. Huang, J.E. Segall, M.M. Wu, Microfluidic modeling of the biophysical microenvironment in tumor cell invasion, Lab Chip 17 (2017) 3221–3233.

[2] D. Wirtz, K. Konstantopoulos, P.C. Searson, The physics of cancer: the role of physical interactions and mechanical forces in metastasis, Nat. Rev. Cancer 11 (2011) 512–522.

[3] N. Gomes, M. Berard, J. Vassy, N. Peyri, C. Legrand, F. Fauvel-Lafeve, Shear stress modulates tumour cell adhesion to the endothelium, Biorheology 40 (2003) 41–45.

[4] G. Follain, N. Osmani, A.S. Azevedo, G. Allio, L. Mercier, M.A. Karreman, G. Solecki, M.J.G. Leon, O. Lefebvre, N. Fekonja, C. Hille, V. Chabannes, G. Dolle, T. Metivet, F.D. Hovsepian, C.

Prudhomme, A. Pichot, N. Paul, R. Carapito, S. Bahram, B. Ruthensteiner, A. Kemmling, S. Siemonsen, T. Schneider, J. Fiehler, M. Glatzel, F. Winkler, Y. Schwab, K. Pantel, S. Harlepp, J.G. Goetz, Hemodynamic forces tune the arrest, adhesion, and extravasation of circulating tumor cells, Dev. Cell 45 (2018) 33–52.

[5] N.Y. Xiong, S. Li, K. Tang, H.X. Bai, Y.T. Peng, H. Yang, C.H. Wu, Y.Y. Liu, Involvement of caveolin-1 in low shear stress-induced breast cancer cell motility and adhesion: roles of FAK/Src and ROCK/p-MLC pathways, BBA-Mol Cell Res 1864 (2017) 12–22.

[6] H.J. Lee, M.F. Diaz, K.M. Price, J.A. Ozuna, S.L. Zhang, E.M. Sevick-Muraca, J.P. Hagan, P.L. Wenzel, Fluid shear stress activates YAP1 to promote cancer cell motility, Nat. Commun. 8 (2017) 14122.

[7] W.T. Chao, J. Kunz, Focal adhesion disassembly requires clathrin-dependent endocytosis of integrins, FEBS Lett. 583 (2009) 1337–1343.

[8] P.Y. Kozyulina, Y.V. Loskutov, V.K. Kozyreva, A. Rajulapati, R.J. Ice, B.C. Jones, E.N. Pugacheva, Prometastatic NEDD9 regulates individual cell migration via caveolin-1-dependent trafficking of integrins, Mol. Cancer Res. 13 (2015) 423–438.

[9] A. Arjonen, J. Alanko, S. Veltel, J. Ivaska, Distinct recycling of active and inactive beta 1 integrins, Eur. J. Cancer 48 (2012) S116.

[10] B.C. Gao, T.M. Curtis, F.A. Blumenstock, F.L. Minnear, T.M. Saba, Increased recycling of alpha 5 beta 1 integrins by lung endothelial cells in response to tumor necrosis factor, J. Cell Sci. 113 (2000) 247–257.

[11] G.K. Xu, C. Yang, J. Du, X.Q. Feng, Integrin activation and internalization mediated by extracellular matrix elasticity: a biomechanical model, J. Biomech. 47 (2014) 1479–1484.

[12] J. Du, X.F. Chen, X.D. Liang, G.Y. Zhang, J. Xu, L.R. He, Q.Y. Zhan, X.Q. Feng, S. Chien, C. Yang, Integrin activation and internalization on soft ECM as a mechanism of induction of stem cell differentiation by ECM elasticity, P Natl Acad Sci USA 108 (2011) 9466–9471.

[13] J. Li, H.R. Chen, Y. Xu, J.L. Hu, F.Q. Xie, C. Yang, Integrin endocytosis on elastic substrates mediates mechanosensing, J. Biomech. 49 (2016) 2644–2654.

[14] G. Apodaca, Endocytic traffic in polarized epithelial cells: role of the actin and microtubule cytoskeleton, Traffic 2 (2001) 149–159.

[15] B. Qualmann, H. Mellor, Regulation of endocytic traffic by rho GTPases, Biochem. J. 371 (2003) 233–241.

[16] S. Mayor, R.E. Pagano, Pathways of clathrin-independent endocytosis, Nat Rev Mol Cell Bio 8 (2007) 603–612.

[17] J.W. Hammond, C.F. Huang, S. Kaech, C. Jacobson, G. Banker, K.J. Verhey, Posttranslational modifications of tubulin and the polarized transport of kinesin-1 in neurons, Mol. Biol. Cell 21 (2010) 572–583.

[18] R. Bhuwania, A. Castro-Castro, S. Linder, Microtubule acetylation regulates dynamics of KIF1C-powered vesicles and contact of microtubule plus ends with podosomes, Eur. J. Cell Biol. 93 (2014) 424–437.

[19] M. Sirajuddin, L.M. Rice, R.D. Vale, Regulation of microtubule motors by tubulin isotypes and post-translational modifications, Nat. Cell Biol. 16 (2014) 335–344.

[20] F. Zhao, L. Li, L. Guan, H. Yang, C. Wu, Y. Liu, Roles for GP IIb/IIIa and alphavbeta3 integrins in MDA-MB-231 cell invasion and shear flow-induced cancer cell mechanotransduction, Cancer Lett. 344 (2014) 62–73.

[21] N.O. Deakin, C.E. Turner, Paxillin inhibits HDAC6 to regulate microtubule acetylation, Golgi structure, and polarized migration, J Cell Biol 206 (2014) 395–413.

[22] A. Hamadi, M. Bouali, M. Dontenwill, H. Stoeckel, K. Takeda, P. Ronde, Regulation of focal adhesion dynamics and disassembly by phosphorylation of FAK at tyrosine 397, J. Cell Sci. 118 (2005) 4415–4425.

[23] P.A. Reid, C. Watts, Cycling of cell-surface MHC glycoproteins through primaquinesensitive intracellular compartments, Nature 346 (1990) 655–657.

[24] F. Shi, J. Sottile, Caveolin-1-dependent beta 1 integrin endocytosis is a critical regulator of fibronectin turnover, J. Cell Sci. 121 (2008) 2360–2371.

[25] T. Pellinen, S. Tuomi, A. Arjonen, M. Wolf, H. Edgren, H. Meyer, R. Grosse, T. Kitzing, J.K. Rantala, O. Kallioniemi, R. Fassler, M. Kallio, J. Ivaska, Integrin trafficking regulated by Rab21 is necessary for cytokinesis, Dev. Cell 15 (2008) 371–385.

[26] R.K. Assoian, M.A. Schwartz, Coordinate signaling by integrins and receptor tyrosine kinases in the regulation of G(1) phase cell-cycle progression, Curr. Opin. Genet. Dev. 11 (2001) 48–53.

[27] K.M. Yamada, S. Even-Ram, Integrin regulation of growth factor receptors, Nat. Cell Biol. 4 (2002) E75–E76.

[28] K.M. Yamada, Integrin signaling, Matrix Biol. 16 (1997) 137–141.

[29] J. Yang, L. Zhu, H. Zhang, J. Hirbawi, K. Fukuda, P. Dwivedi, J.M. Liu, T. Byzova, E.F. Plow, J.H. Wu, J. Qin, Conformational activation of talin by RIAM triggers integrin-mediated cell adhesion, Nat. Commun. 5 (2014) 5880.

[30] A. Tiwari, J.J. Jung, S.M. Inamdar, C.O. Brown, A. Goel, A. Choudhury, Endothelial cell migration on fibronectin is regulated by syntaxin 6-mediated alpha 5 beta 1 integrin recycling, J. Biol. Chem. 286 (2011) 36749–36761.

[31] H. Yang, L. Guan, S. Li, Y. Jiang, N. Xiong, L. Li, C. Wu, H. Zeng, Y. Liu, Mechanosensitive caveolin-1 activation-induced PI3K/Akt/mTOR signaling pathway promotes breast cancer motility, invadopodia formation and metastasis in vivo, Oncotarget 7 (2016) 16227–16247.

[32] J.A. Broussard, D.J. Webb, I. Kaverina, Asymmetric focal adhesion disassembly in motile cells, Curr. Opin. Cell Biol. 20 (2008) 85–90.

[33] D. Valdembri, G. Serini, Regulation of adhesion site dynamics by integrin traffic, Curr. Opin. Cell Biol. 24 (2012) 582–591.

[34] D.I. Mundy, T. Machleidt, Y.S. Ying, R.G.W. Anderson, G.S. Bloom, Dual control of caveolar membrane traffic by microtubules and the actin cytoskeleton, J. Cell Sci. 115 (2002) 4327–4339.

[35] R.G. Parton, B. Joggerst, K. Simons, Regulated internalization of caveolae, J. Cell Biol. 127 (1994) 1199–1215.

[36] S.A. Wickstrom, A. Lange, M.W. Hess, J. Polleux, J.P. Spatz, M. Kruger, K. Pfaller, A. Lambacher, W. Bloch, M. Mann, L.A. Huber, R. Fassler, Integrin-linked kinase controls microtubule dynamics required for plasma membrane targeting of caveolae, Dev. Cell 19 (2010) 574–588.

[37] A. Echarri, M.A. Del Pozo, Caveolae - mechanosensitive membrane invaginations linked to actin filaments, J. Cell Sci. 128 (2015) 2747–2758.

[38] A. Matov, K. Applegate, P. Kumar, C. Thoma, W. Krek, G. Danuser, T. Wittmann, Analysis of microtubule dynamic instability using a plus-end growth marker, Nat. Methods 7 (2010) 761–768.

[39] R. Takemura, S. Okabe, T. Umeyama, Y. Kanai, N.J. Cowan, N. Hirokawa, Increased microtubule stability and alpha tubulin acetylation in cells transfected with microtubule-associated proteins MAP1B, MAP2 or tau, J Cell Sci 103 (Pt 4) (1992) 953–964.

[40] T. Shida, J.G. Cueva, Z. Xu, M.B. Goodman, M.V. Nachury, The major alpha-tubulin K40 acetyltransferase alphaTAT1 promotes rapid ciliogenesis and efficient mechanosensation, Proc. Natl. Acad. Sci. U. S. A. 107 (2010) 21517–21522.

[41] C. Creppe, L. Malinouskaya, M.L. Volvert, M. Gillard, P. Close, O. Malaise, S. Laguesse, I. Cornez, S. Rahmouni, S. Ormenese, S. Belachew, B. Malgrange, J.P. Chapelle, U. Siebenlist, G. Moonen, A. Chariot, L. Nguyen, Elongator controls the migration and differentiation of cortical neurons through acetylation of alphatubulin, Cell 136 (2009) 551–564.

[42] Q.Q. Zuo, W.J. Wu, X. Li, L. Zhao, W. Chen, HDAC6 and SIRT2 promote bladder cancer cell migration and invasion by targeting cortactin, Oncol. Rep. 27 (2012) 819–824.

[43] J. Asthana, S. Kapoor, R. Mohan, D. Panda, Inhibition of HDAC6 deacetylase activity increases its binding with microtubules and suppresses microtubule dynamic instability in MCF-7 cells, J. Biol. Chem. 288 (2013) 22516–22526.

[44] A.V. Schofield, R. Steel, O. Bernard, Rho-associated coiled-coil kinase (ROCK) protein controls microtubule dynamics in a novel signaling pathway that regulates cell migration, J. Biol. Chem. 287 (2012) 43620–43629.

[45] M. Rey, M. Irondelle, F. Waharte, F. Lizarraga, P. Chavrier, HDAC6 is required for invadopodia activity and invasion by breast tumor cells, Eur. J. Cell Biol. 90 (2011) 128–135.

[46] K. Kanno, S. Kanno, H. Nitta, N. Uesugi, T. Sugai, T. Masuda, G. Wakabayashi, C. Maesawa, Overexpression of histone deacetylase 6 contributes to accelerated migration and invasion activity of hepatocellular carcinoma cells, Oncol. Rep. 28 (2012) 867–873.

[47] V.A. Morikis, S. Chase, T. Wun, E.L. Chaikof, J.L. Magnani, S.I. Simon, Selectin catch-bonds mechanotransduce integrin activation and neutrophil arrest on inflamed endothelium under shear flow, Blood 130 (2017) 2101–2110.

[48] F. Fang, S.M. Wasserman, J. Torres-Vazquez, B. Weinstein, F. Cao, Z. Li, K.D. Wilson, W. Yue, J.C. Wu, X. Xie, X. Pei, The role of Hath6, a newly identified shear-stress-responsive transcription factor, in endothelial cell differentiation and function, J. Cell Sci. 127 (2014) 1428–1440.

[49] S. Li, Y. Chen, Y. Zhang, X. Jiang, Y. Jiang, X. Qin, H. Yang, C. Wu, Y. Liu, Shear stress promotes anoikis resistance of cancer cells via caveolin-1-dependent extrinsic and intrinsic apoptotic pathways, J. Cell. Physiol. 234 (2018) 3730–3743.

[50] P. Caswell, J. Norman, Endocytic transport of integrins during cell migration and invasion, Trends Cell Biol. 18 (2008) 257–263.

[51] C. Urbich, D.H. Walter, A.M. Zeiher, S. Dimmeler, Laminar shear stress upregulates integrin expression - role in endothelial cell adhesion and apoptosis, Circ. Res. 87 (2000) 683–689.

[52] Z.Z. Gu, E.H. Noss, V.W. Hsu, M.B. Brenner, Integrins traffic rapidly via circular dorsal ruffles and macropinocytosis during stimulated cell migration, J. Cell Biol. 193 (2011) 61–70.

[53] N.D. Boyd, B.M.C. Chan, N.O. Petersen, Adaptor protein-2 exhibits alpha(1)beta(1) or alpha(6)beta(1) integrin-dependent redistribution in rhabdomyosarcoma cells, Biochemistry-Us 41 (2002) 7232–7240.

[54] J. Teichmann, A. Morgenstern, J. Seebach, H.J. Schnittler, C. Werner, T. Pompe, The control of endothelial cell adhesion and migration by shear stress and matrixsubstrate anchorage, Biomaterials 33 (2012) 1959–1969.

[55] D. Verma, F.J. Meng, F. Sachs, S.Z. Hua, Flow-induced focal adhesion remodeling mediated by local cytoskeletal stresses and reorganization, Cell Adhes. Migr. 9 (2015) 432–440.

[56] Z.D. Nassar, M.M. Hill, R.G. Parton, M. Francois, M.O. Parat, Non-caveolar caveolin-1 expression in prostate cancer cells promotes lymphangiogenesis, Oncoscience 2 (2015) 635–645.

[57] L. Nimri, H. Barak, L. Graeve, B. Schwartz, Restoration of caveolin-1 expression suppresses growth, membrane-type-4 metalloproteinase expression and metastasisassociated activities in colon cancer cells, Mol. Carcinog. 52 (2013) 859–870.

[58] M. Sung, X. Tan, B. Lu, J. Golas, C. Hosselet, F. Wang, L. Tylaska, L. King, D. Zhou, R. Dushin, J.S. Myers, E. Rosfjord, J. Lucas, H.P. Gerber, F. Loganzo, Caveolaemediated endocytosis as a novel mechanism of resistance to trastuzumab emtansine (T-DM1), Mol. Cancer Ther. 17 (2018) 243–253.

[59] F. Meng, S. Saxena, Y. Liu, B. Joshi, T.H. Wong, J. Shankar, L.J. Foster, P. Bernatchez, I.R. Nabi, The phospho-caveolin-1 scaffolding domain dampens force fluctuations in focal adhesions and promotes cancer cell migration, Mol. Biol. Cell 28 (2017) 2190–2201.

[60] B. Joshi, J. Pawling, J. Shankar, K. Pacholczyk, Y. Kim, W. Tran, F. Meng, A.M.A. Rahman, L.J. Foster, H.S. Leong, J.W. Dennis, I.R. Nabi, Caveolin-1 Y14 phosphorylation suppresses tumor growth while promoting invasion, Oncotarget 10 (2019) 6668–6677.

[61] M. Nethe, P.L. Hordijk, A model for phospho-caveolin-1 driven turnover of focal adhesions, Cell Adhes. Migr. 5 (2011) 59–64.

[62] Y.H. Wang, Z.Q. Yan, Y.X. Qi, B.B. Cheng, X.D. Wang, D. Zhao, B.R. Shen, Z.L. Jiang, Normal shear stress and vascular smooth muscle cells modulate migration of endothelial cells through histone deacetylase 6 activation and tubulin acetylation, Ann. Biomed. Eng. 38 (2010) 729–737.

[63] A. Echarri, O. Muriel, D.M. Pavon, H. Azegrouz, F. Escolar, M.C. Terron, F. SanchezCabo, F. Martinez, M.C. Montoya, O. Llorca, M.A. del Pozo, Caveolar domain organization and trafficking is regulated by Abl kinases and mDia1, J. Cell Sci. 125 (2012) 3097–3113.

[64] S. Stehbens, T. Wittmann, Targeting and transport: how microtubules control focal adhesion dynamics, J. Cell Biol. 198 (2012) 481–489.

[65] L. Zhang, N. Liu, S. Xie, X. He, J. Zhou, M. Liu, D. Li, HDAC6 regulates neuroblastoma cell migration and may play a role in the invasion process, Cancer Biol Ther 15 (2014) 1561–1570.

[66] K.J. Verhey, J.W. Hammond, Traffic control: regulation of kinesin motors, Nat Rev Mol Cell Bio 10 (2009) 765–777.

[67] T. Yamamoto, Y. Ugawa, M. Kawamura, K. Yamashiro, S. Kochi, H. Ideguchi, S. Takashiba, Modulation of microenvironment for controlling the fate of periodontal ligament cells: the role of Rho/ROCK signaling and cytoskeletal dynamics, J Cell Commun Signal 12 (2018) 369–378.

[68] K. Savage, M.B. Lambros, D. Robertson, R.L. Jones, C. Jones, A. Mackay, M. James, J.L. Hornick, E.M. Pereira, F. Milanezi, C.D. Fletcher, F.C. Schmitt, A. Ashworth, J.S. Reis-Filho, Caveolin 1 is overexpressed and amplified in a subset of basal-like and metaplastic breast carcinomas: a morphologic, ultrastructural, immunohistochemical, and in situ hybridization analysis, Clin Cancer Res 13 (2007) 90–101.

[69] B. Joshi, S.S. Strugnell, J.G. Goetz, L.D. Kojic, M.E. Cox, O.L. Griffith, S.K. Chan, S.J. Jones, S.P. Leung, H. Masoudi, S. Leung, S.M. Wiseman, I.R. Nabi, Phosphorylated caveolin-1 regulates Rho/ROCK-dependent focal adhesion dynamics and tumor cell migration and invasion, Cancer Res. 68 (2008) 8210–8220.

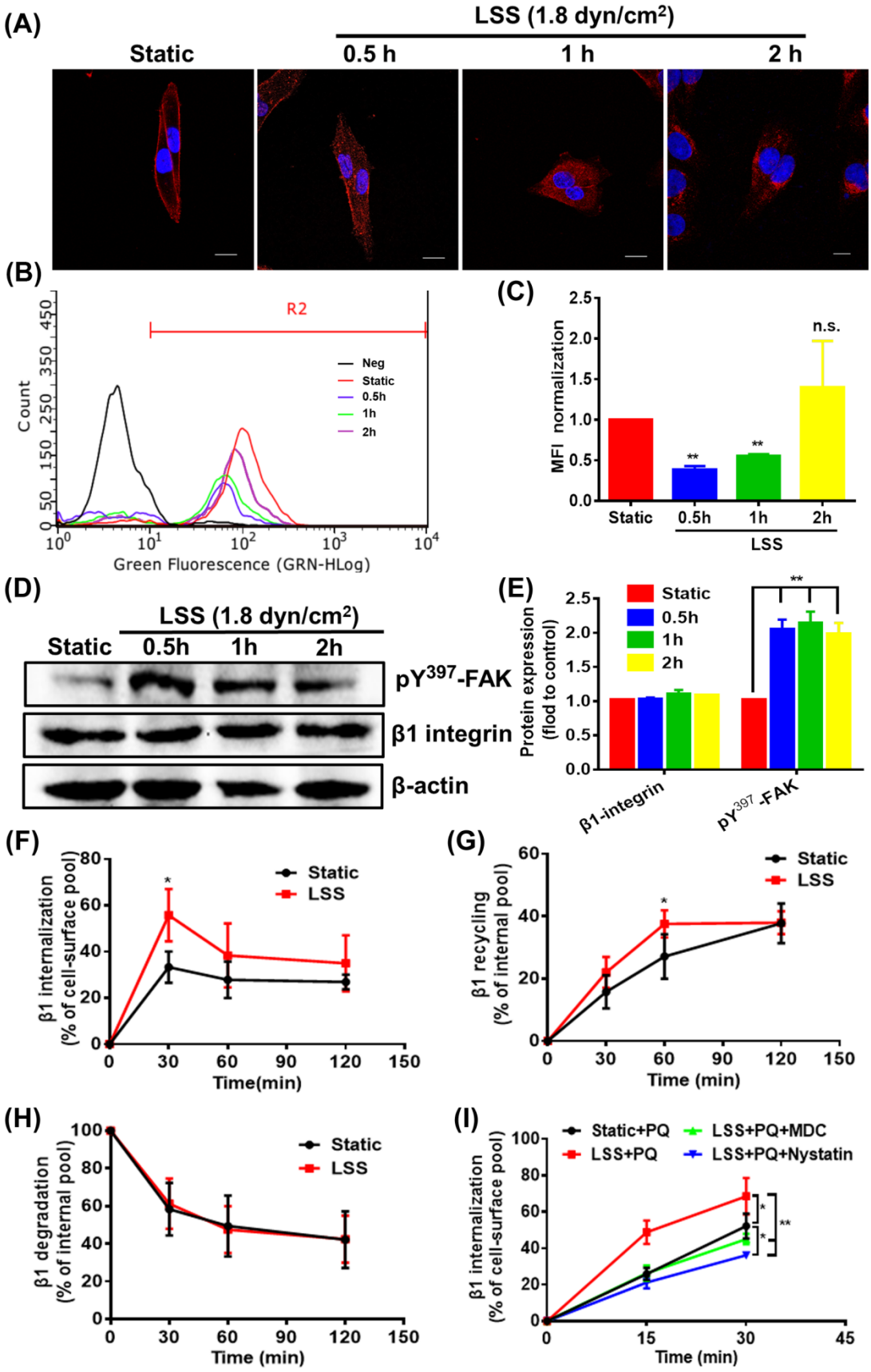

Fig.1. Low shear stress (LSS) promotes integrin β1 internalization and recycling in MDA-MB-231 cells. (**A**) Distribution of integrin β1 in response to

LSS. MDA-MB-231 cells were seeded on glass slips. Adherent cells were kept under static condition as control or exposed to LSS (1.8 dyn/cm^2) for the indicated durations. The cells were fixed with 4% paraformaldehyde and stained for DNA (blue) and integrin β1 (red). Scale bar = 10 μm. (**B**) Redistribution of integrin β1 on the cell surface was determined by FACS. (**C**) Quantification of mean fluorescence intensities (MFI) from (B). (**D**) LSS enhances FAK phosphorylation but not integrin β1 expression. The total amount of Integrin β1 and FAK activation were analyzed by western blotting assay in cells treated by LSS. (**E**) Quantification of integrin β1 expression and FAK activation normalized to β-actin from (D). Internalization of integrin β1 (**F**), recycling of internalized integrin β1 (**G**), and degradation of internalized integrin β1 (**H**) in response to static condition or LSS (1.8 dyn/cm^2). These responses were determined by capture-ELISA. (**I**) LSS enhances internalization of integrin β1 through clathrin and no clathrin-dependent pathways. Cells were pretreated with nystatin (100 μM) or MDC (50 μM) for 1h, and then exposed to static condition or LSS (1.8 dyn/cm^2) in the presence of 0.6 mM primaquine (PQ). Net internalization of integrin β1 was determined by capture-ELISA. PQ was used to block the endosomal recycling of integrins. MDC and nystatin were used to block clathrin-dependent and Cav-1-dependent internalization, respectively. All the values represent mean ± SD from three independent experiments. *$p<0.05$, **$p<0.01$, n.s., no significance.

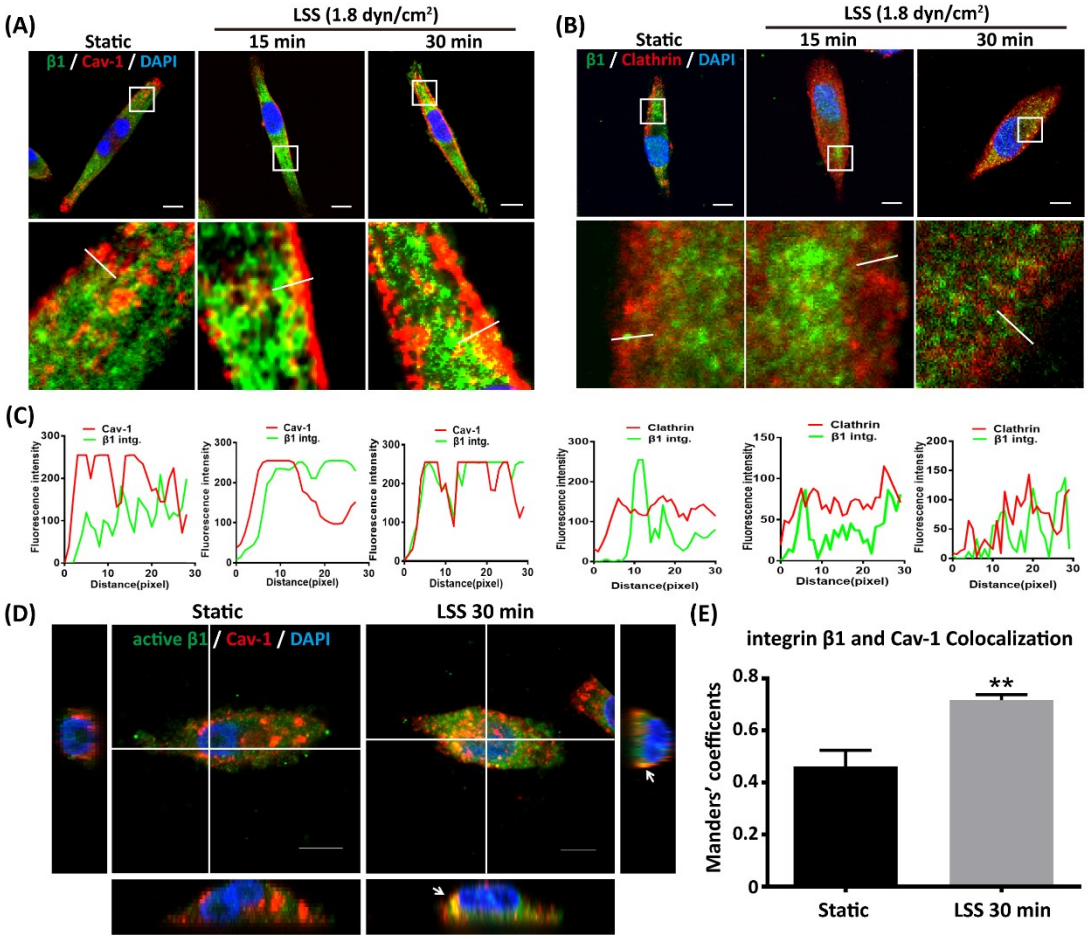

Fig.2. Co-localization of Cav-1 and integrin β1 during LSS accelerates integrin internalization. The colocalization of integrin β1 and Cav-1 (**A**) and of integrin β1 and clathrin (**B**) in LSS-treated cells. MDA-MB-231 Cells were seeded on glass slides. Adherent cells were kept under static condition as control or exposed to LSS (1.8 dyn/cm^2) for the indicated durations and fixed with 4% paraformaldehyde. The colocalization of integrin β1 and clathrin or Cav-1 was examined by confocal imaging. The cells were stained for DAPI (blue), integrin β1 (green) and clathrin or Cav-1 (red). Bottom panels show an enlargement of the area indicated by the white rectangle in the top panels. Scale bars=10 μm. (**C**) Fluorescence intensity profiles show the colocalization of integrin β1 and Cav-1 but not clathrin. The fluorescence intensities from the lines indicated in (**A)** and **(B)** were analyzed by Image Pro Plus software. (**D**) The colocalization of active integrin β1 and Cav-1. Active integrin β1 (green), Cav-1 (red), and DAPI (blue) were stained by immunofluorescence and imaged by confocal microscopy. The white arrows indicate the areas positive for active integrin β1 and Cav-1. Scale bar=10 μm. (**E**) Quantification of the colocalization of active integrin β1 and Cav-1 in (**D)**. Histograms show mean ± SD of colocalization over the whole image as PC coefficients (n=5).

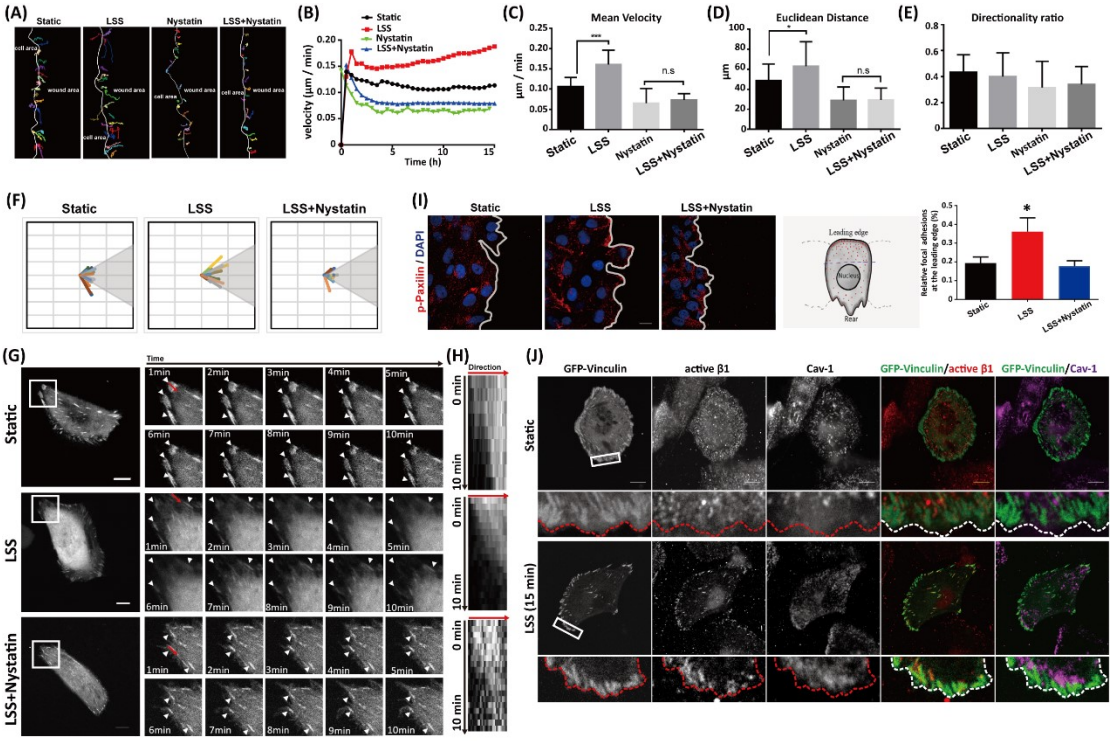

Fig.3. Clathrin-independent internalization is necessary for LSS-induced directional cell migration, FA disassembly and polarized FAs assembly. (**A**) Inhibiting clathrin-independent internalization blocks LSS-induced cell migration. Cell monolayers were pretreated with nystatin (100 μM, 1 h) or DMSO and kept under static condition as control or exposed to LSS (1.8 dyn/cm^2) in the presence of nystatin for 2 h. These cells were then wounded with a pipet tip and migration was recorded by time-lapse video microscopy (total 15 h, 15-min frame interval). Cell tracks were determined using the Image J software ('Manual Tracking' plug-in). Tracks of single cells at the wounded edge were shown. The wound edge was indicated by a white line. (**B**) Quantification of instant velocity in (**A**). Cell migration velocity was analyzed for each group and plotted as a function of time (0-15 h). (**C**-**E**) Quantification of the mean velocity, Euclidean distance, and Directionality ratio in (**A**). (**F**) Percentage of cells with within a 60° angle of directionality migration in (A). (**G**) Time-lapsed photomicrographs of FAs in MDA-MB-231 cells. GFP-vinculin cells were pretreated with nystatin (100 μM, 1 h) or DMSO, and then kept under static condition as control or exposed to LSS (1.8 dyn/cm^2) in the presence of nystatin for 2 h before imaging (30 s intervals over a 10 min time course). The

outlined regions in the left panel were enlarged in the right panels at the indicated time points. Scale bar=10 μm. (**H**) Kymographs taken along red lines in (**G**) show FAs disassembly. (**I**) Inhibiting clathrin-independent internalization blocks LSS-induced FA polarized assembly. MDA-MB-231 were pretreated with nystatin (100 μM, 1h) or DMSO and kept static as control or exposed to LSS (1.8 dyn/cm^2, 2 h) in the presence of nystatin. p-Paxillin (red) and DNA (blue) in wounded monolayers were examined by immunofluorescence. Scale bar=20 μm. (**J**) LSS induces the colocalization of vinculin and active integrin β1, and stimulates the accumulation of Cav-1 next to the FAs on the cell edge. GFP-vinculin cells were kept under static condition as control or exposed to LSS (1.8 dyn/cm^2, 15min) and fixed with 4% paraformaldehyde. The cells were stained for active integrin β1 (red) and Cav-1 (magenta), and imaged by confocal microscopy. Bottom panels show an enlargement of the area indicated by the white rectangle in the top panels. Scale bars=10 μm. Data represent mean ± SD of three independent experiments. *$p<0.05$, ***$p<0.001$, n.s., no significant difference.

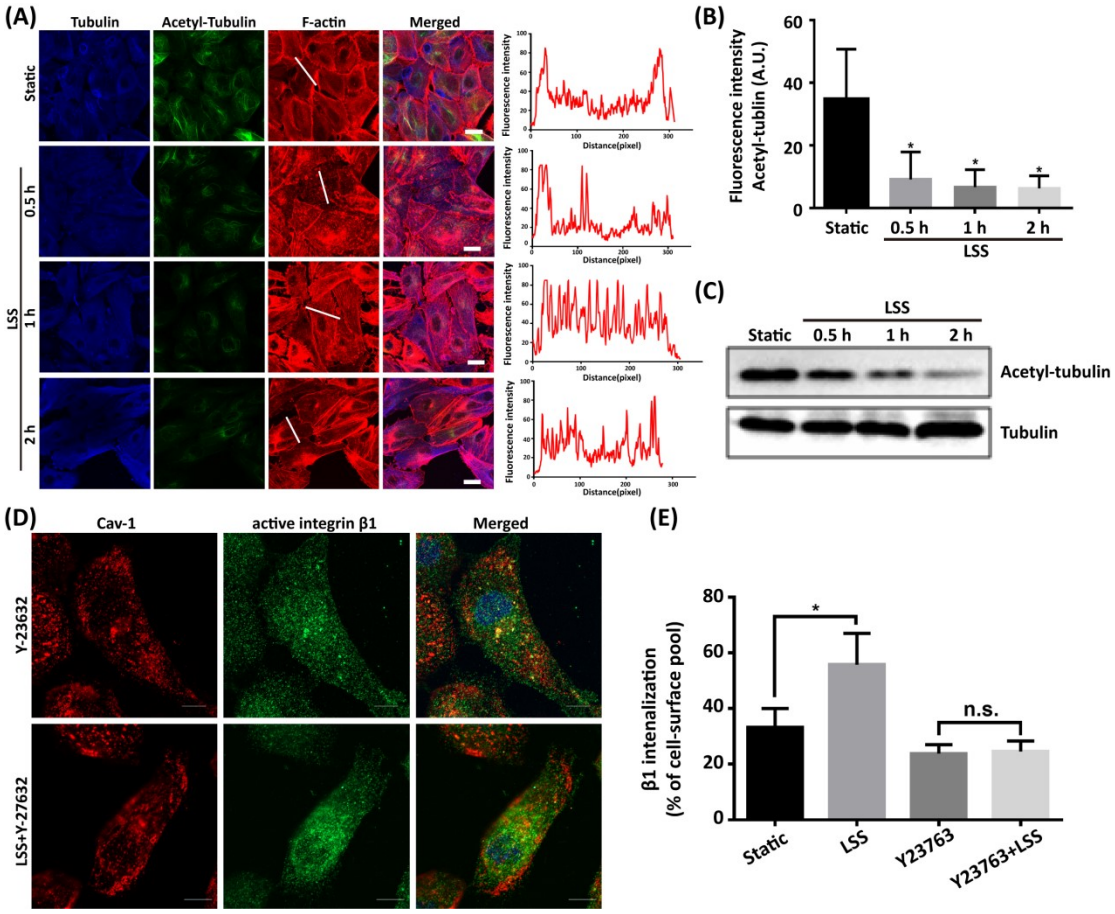

Fig.4. LSS decreases acetylation of tubulin and induces actin cytoskeletal reorganization required for integrin β1 internalization. (**A**) LSS induces tubulin deacetylation and actin reorganization. MDA-MB-231 Cells were kept under static condition as control or exposed to LSS (1.8 dyn/cm^2) for the indicated durations. Fluorescence intensity profiles of F-actin show the actin cytoskeletal reorganization (white lines). The cells were then stained for tubulin (blue), acetyl-tubulin (green) and F-actin (red). Scale bar=10 μm. (**B**) Quantitative analysis of acetyl-tubulin in (**A**). A.U., arbitrary unit. (**C**) LSS decreases tubulin acetylation at the protein level. Western blot analysis was conducted to analyze the acetyl-tubulin levels in MDA-MB-231 cells exposed to LSS (1.8 dyn/cm^2) for the indicated durations. (**D**) Inhibiting ROCK blocks the LSS-induced colocalization of Cav-1 and active integrin β1. Cells were pretreated with ROCK inhibitor Y-27632 (10 μM, 18 h), and then kept under static condition as control or exposed to LSS (1.8 dyn/cm^2) for 30 min. The cells

were fixed with 4% paraformaldehyde then immunostained for DNA (blue), active integrin β1 (green) and Cav-1 (red). (**E**) Inhibiting ROCK suppresses LSS-induced internalization of integrin β1. After cells were pretreated with ROCK inhibitor Y-27632 (10 μM, 18 h), internalization of integrin β1 in static condition or LSS (1.8 dyn/cm^2, 30 min) exposure in the presence of Y-27632 were determined by capture-ELISA. Data represent mean ± SD of three independent experiments.*$p<0.05$, n.s., no significant difference.

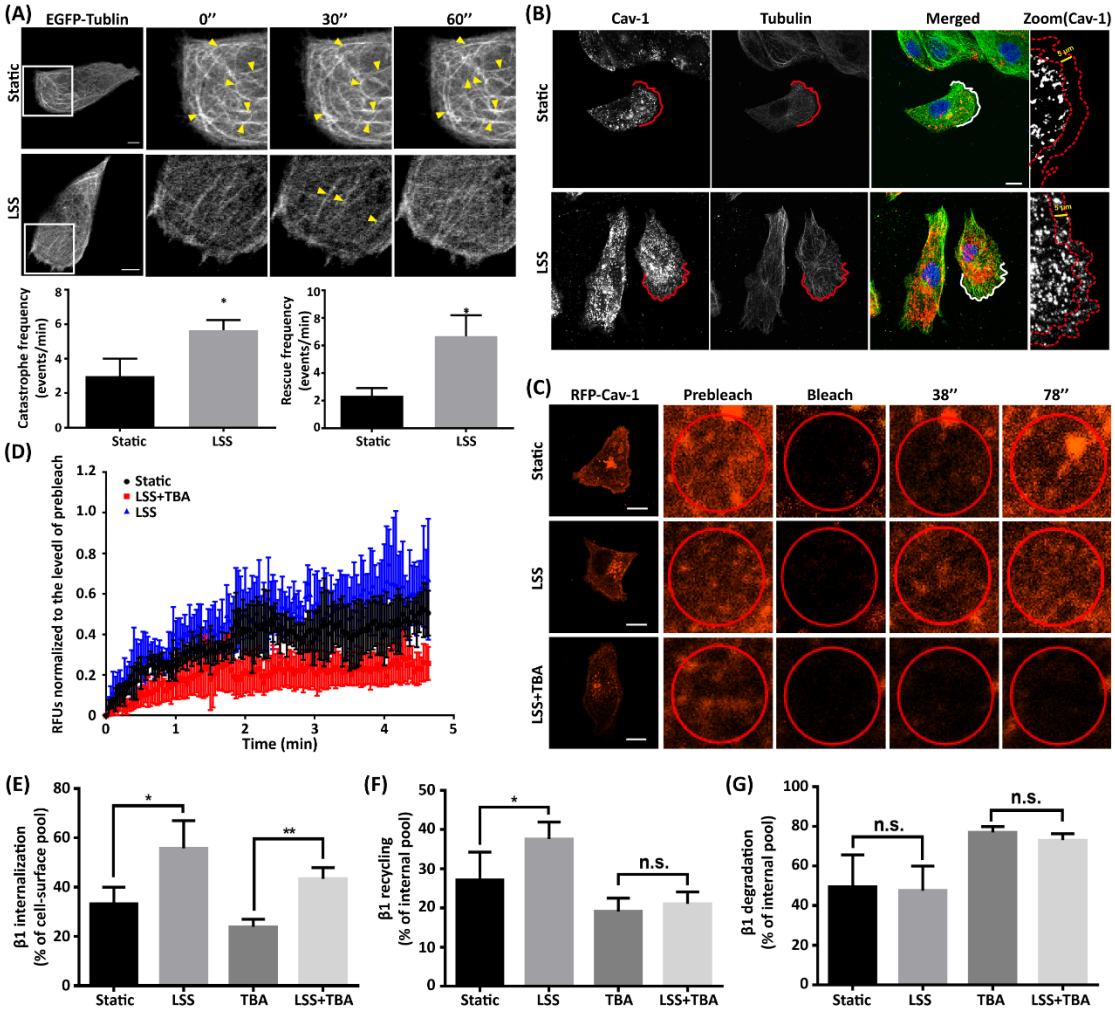

Fig.5. LSS-induced tubulin deacetylation enhances MT dynamics, Cav-1 motility, and integrin β1 recycling. (**A**) LSS promotes MT dynamics. EGFP-tubulin MDA-MB-231 cells were kept under static condition as control or exposed to LSS (1.8 dyn/cm^2) for 2 h. Dynamics of MTs were analyzed by confocal microscopy. Images were acquired every 10 s for 3 min. Right panels show an enlargement of the area indicated by the white rectangle in the left panels. Lower panels show the the quantitative analysis of MT dynamics. Arrows denote stable MTs. Scale bar=10 μm. (**B**) LSS facilitates the recruitment of Cav-1 to peripheral MTs at the leading edge of cells. Cells were kept under static condition as control or exposed to LSS (1.8 dyn/cm^2) for 2 h. The cells were fixed with 4% paraformaldehyde and stained for DNA (blue), tubulin (green), and Cav-1 (red). Right panels show an enlargement of the area indicated by the white rectangle. Dotted line show the cell edge, * show the area without Cav-1 signal. Scale bar = 10 μm. (**C**) LSS enhances Cav-1 mobility. MDA-MB-231 cells were transfected with RFP-Cav-1 plasmid and pretreated with HDAC6 inhibitor TBA (10 μM, 18 h). These cells were kept under static condition as control or exposed to LSS (1.8 dyn/cm^2) in the presence of TBA for 2 h before FRAP analysis of RFP-Cav-1 mobility. Right panels show an enlargement of the area indicated by the white rectangle.

From left to right, prebleach, bleach, and 38 s, 78 s after bleaching were shown. The red circles indicate the bleached areas. Scale bar=10 μm. (**D**) Quantification of FRAP analysis in (**C**). Fluorescence recovery was recorded every 2 s for 5 min. The data represent mean ± SD of three independent experiments. LSS-induced tubulin deacetylation blocks integrin β1 recycling (**F**) but not internalization (**E**) and degradation (**G**). After cells were pretreated with TBA (10 μM, 16 h), internalization, recycling, and degradation of integrin β1 in static condition or LSS (1.8 dyn/cm^2, 30min) exposure in the presence of TBA were determined by capture-ELISA. Data represent mean ± SD of three independent experiments.*p<0.05, **p<0.01, n.s., no significant difference.

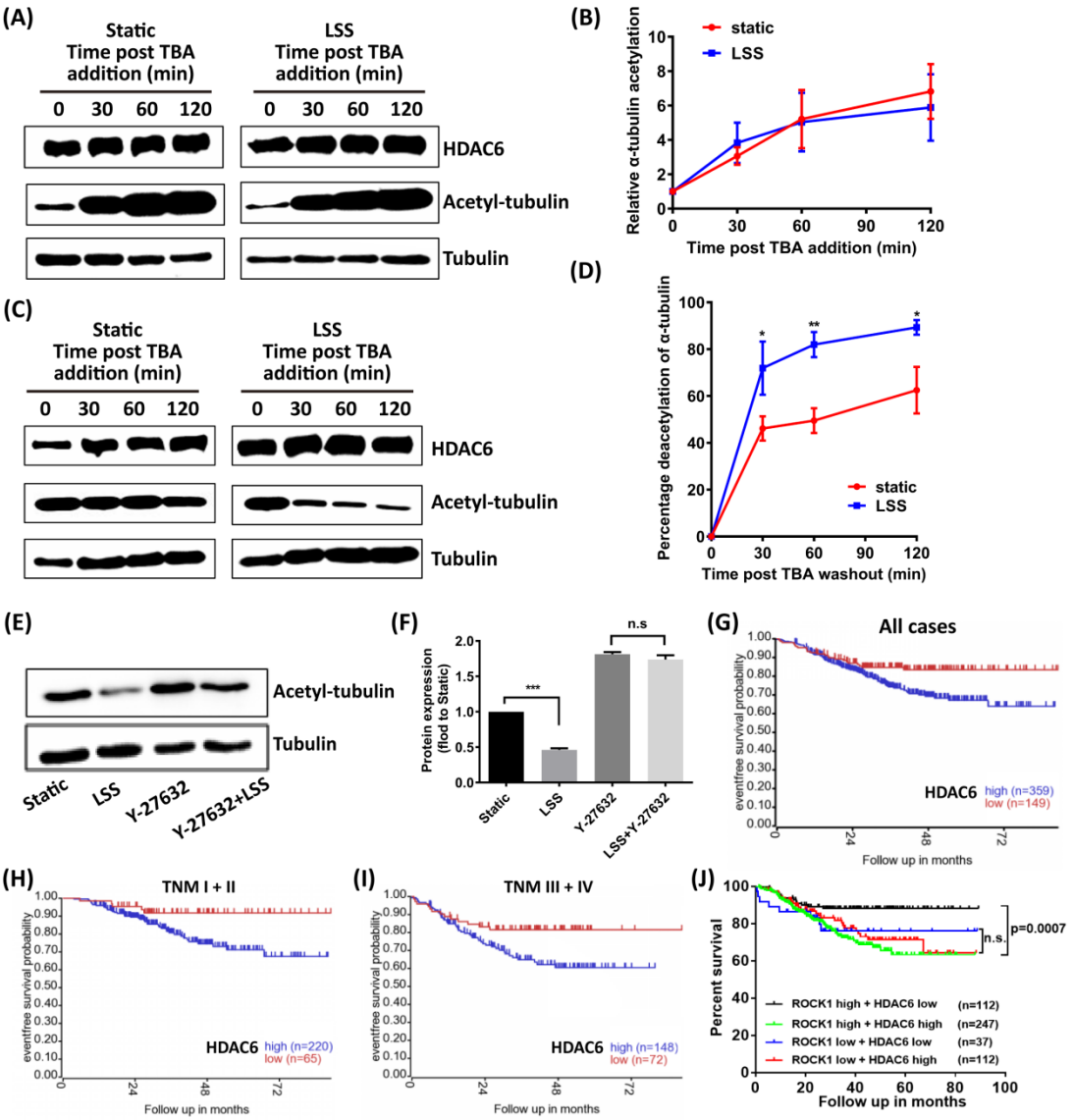

Fig.6. ROCK-dependent activation of HDAC6 is required for LSS-induced MT deacetylation. (**A**) Inhibiting HDAC6 blocks LSS-induced MT deacetylation. MDA-MB-231 cells were treated with TBA (10 μM) and kept under static condition as control or exposed to LSS (1.8 dyn/cm^2) for the indicated durations. The α-tubulin acetylation was measured by western blot analysis. (**B**) Quantification of acetyl-tubulin normalized to α-tubulin in (**A**). (**C**) HDAC6 mediates LSS-induced MT deacetylation. Cells were pretreated with TBA (10 μM) for 16 h. After the TBA-containing medium was replaced by fresh medium, the cells were kept under static condition or exposed to LSS (1.8 dyn/cm^2) for the indicated durations. The α-tubulin deacetylation was measured by western blot analysis. (**D**) Quantification of acetyl-tubulin normalized to α-tubulin in (**C**).

(**E**) Inhibiting ROCK blocks LSS-induced MT deacetylation. Cells were pretreated with Y-27632 (10 μM) for 18 h and then kept under static condition as control or exposed to LSS (1.8 dyn/cm^2) for 2 h in the presence of Y-27632. The acetyl-tubulin levels were measured by western blot analysis. (**F**) Quantification of acetyl-tubulin levels normalized to α-tubulin in (**E**). Data represent mean ± SD of three independent experiments. *p<0.05,**p<0.01, ***p<0.001, n.s., no significant difference. Kaplan-Meier analysis of survival rate based on HDAC6 expression in all (**G**), TNM I+II (**H**) and TNM III+IV (**I**) breast cancer patients treated with chemotherapy drugs taxane and anthracycline. The blue and red line represents high and low HDAC6 mRNA expression, respectively. (**J**) Kaplan-Meier analysis of survival rate based on the combination of HDAC6 and ROCK1 expression in all breast cancer patients treated with chemotherapy drugs taxane and anthracycline. n.s., no significant difference; all p-values were calculated by log-rank test.

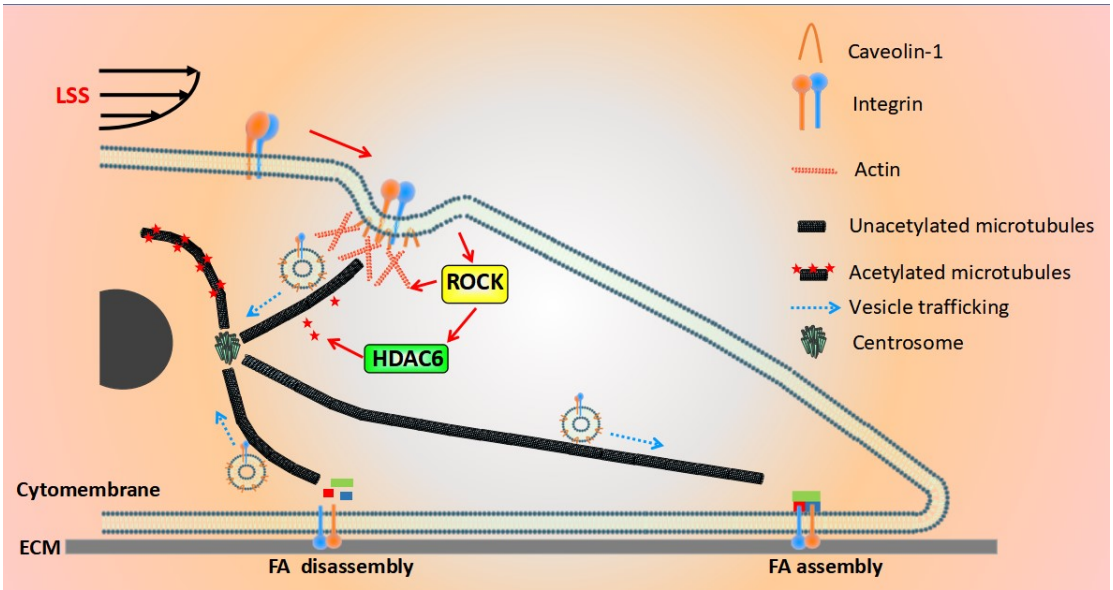

Fig.7. Schematic summary of Shear stress stimulates Integrin β1 trafficking and increases directional migration of cancer cells *via* promoting deacetylation of microtubule. LSS could trigger ROCK-mediated actin cytoskeletal reorganization to facilitate Cav-1 redistribution and integrin β1 internalization, which promotes the disassembly of FAs. LSS-activated ROCK/HDAC6 pathway could decrease acetylation of MT, resulting in enhanced MT dynamics, Cav-1 motility and integrin β1 recycling. In summary, LSS increases integrin β1 trafficking, Cav-1 redistribution, FA dynamics, and Cav-1 motility, which further facilitate directional cell migration.